

Microcluster Growth: Transition from Successive Monomer Addition to Coagulation

J. M. Soler and N. García

Departamento de Física Fundamental, Universidad Autónoma de Madrid, Canto Blanco, Madrid 34, Spain

and

O. Echt, K. Sattler, and E. Recknagel

Fakultät für Physik, Universität Konstanz, D-7750 Konstanz, West Germany

(Received 30 March 1982)

The transition in cluster growth from successive monomer absorption to cluster coalescence has been observed for CO_2 condensed in a supersonic beam under high pressure. A model which considers all cluster-cluster reactions achieves good qualitative agreement with the measured size distributions of the clusters. This is the first attempt to fit an experimental cluster spectrum from a first-principles model.

PACS numbers: 64.70.Fx, 05.20.Dd, 36.40.+d

In this paper growth of matter in its first stages is described. At the beginning successive atom absorption is the leading process, gradually changing to coagulation when the density of clusters is high enough for coalescence. Both processes are characterized by typical size distributions: Steeply, roughly exponentially decreasing size distributions are predicted by nucleation theory if the condensate mass fraction is small¹; this is verified by experiments.² On the other hand, growth of particles by coalescence leads to a Gaussian distribution for the logarithm of the size; this has been shown for particles produced by inert-gas evaporation³ and for island formation in discontinuous films.⁴ However, this so called log-normal size distribution could not be continuously shifted to smaller sizes where its qualitative change is expected. We report on the first observation of this transition and present a model which explains the measured distributions by fitting a single parameter which measures the degree of nucleation.

Supersonic nozzle expansion has been a current tool to study homogeneous nucleation for many years.^{1,5} Much of the interest was devoted to calculating the critical supersaturation at the condensation onset and in most cases the steady-state hypothesis^{6,7} was assumed. Mass spectrometry of the expanded beams has become a current topic.^{2,8} Rather few spectra, however, have been reported for larger clusters (size $i \gtrsim 10^2$ molecules per cluster)^{9,10}; and these spectra are distorted by the occurrence of multiply charged clusters and their fragment ions.^{11,12} No spectra have been reported which demonstrate the qualitative change in the size distributions in the transition from successive monomer absorption to cluster coagulation; and no attempt has been

made to fit a mass spectrum from a first-principles theory. This is mainly because of the enormous difficulty of calculating the thermodynamic properties of the clusters.¹³ In this Letter we present a set of mass spectra of CO_2 clusters which are free of the above-mentioned distortions. The size distributions recorded with high stagnation pressures are no longer compatible with the steady-state hypothesis. Instead, the small clusters decrease in intensity until they completely disappear when the pressure becomes high enough. We also present a model which explains qualitatively the observed mass spectra by a cluster-cluster coagulation mechanism for growth.

The clusters are produced by adiabatic expansion of CO_2 (purity 99.995%) through a capillary (diameter 0.2 mm, length 20 mm) into vacuum; homogeneous nucleation occurs in the supersonic jet.¹⁴ For a given gas, nozzle geometry, and nozzle temperature T_0 , the mean cluster size can be varied by changing the stagnation pressure p_0 . The jet is skimmed by two conical collimators; the pressure behind the nozzle is kept below 10^{-3} mbar by cooling the walls of the expansion chamber with liquid nitrogen. The jet enters the time-of-flight mass spectrometer¹⁵ where it is ionized by a pulsed electron beam with an energy of 35 eV. At this energy double ionization of CO_2 clusters and thus dissociation by Coulomb explosion is avoided.^{11,12} Further reduction of the electron energy down to 25 eV had no effect on the recorded mass spectra.

The ions are axially accelerated to 2 keV and enter a drift tube of length 110 cm. The axial arrangement prevents mass discrimination for large clusters which already have an appreciable kinetic energy in the neutral jet ($E_i \approx 0.07i$ eV where i is the number of molecules in the clus-

ter). On the other hand, the distortion of the linear relation between the time of flight and the square root of the cluster size i is still negligible as long as $i \ll 3 \times 10^4$. At the end of the drift tube, the cluster ions hit the cathode (activated CuBe plate) of a discrete electron multiplier and are detected by single-ion counting. The time elapsed between the pulse of the ionizing electrons and the detector signal is digitized and stored in a multichannel analyzer.

A comparison between a size distribution, calculated for neutral clusters, and a mass spectrum, exploiting electron-impact ionization and single-ion detection, requires knowledge of the size dependences of the ionization cross section, σ_i , and of the detection probability, η_i . σ_i is expected to increase linearly with the geometrical cross section of the cluster, i.e., $\sigma_i \propto i^{2/3}$, if the cluster is sufficiently large ($i \gtrsim 30$).¹⁶ This relation, in accordance with experiments, holds because low-energy electrons can only ionize a surface layer of a large cluster.

In a conventional ion detector, the secondary-electron yield and thus the detection efficiency for cluster ions with kinetic energies in the kiloelectronvolt range decrease with increasing size i .¹⁷ The exact dependence of η_i on i is a sensitive function of various parameters such as the kinetic energy, monomer mass, and state of the target surface. To avoid this complication, we chose a detector design which allows for detection of clusters as large as $i = 10^7$, with an efficiency essentially independent of the cluster size.¹⁰ This is achieved by a grid in front of the cathode. The cluster ions hit the grid with an energy of 2 keV; they immediately boil off most of their neutral molecules, resulting in a small ion which is focused and post-accelerated to the cathode by a potential of 3.5 kV. This process ensures a constant detection probability for large clusters which would remain undetectable without a stripping grid.

Figure 1 displays mass spectra of CO₂ clusters produced by expansion of CO₂ at constant nozzle temperature, $T_0 = 225$ K, but increasing stagnation pressure p_0 . The apparent onset of nucleation occurs at $p_0 \approx 100$ mbar (not shown in Fig. 1). The usual, roughly exponential intensity decrease with increasing size is observed up to 700 mbar. (Our spectrometer resolves individual mass peaks up to $i \approx 100$,¹² but in the reproduction of Fig. 1 they merge into a band.¹⁸) The distributions then gradually become peaked with increasing p_0 . For $p_0 \geq 2000$ mbar, small clusters (apart from the

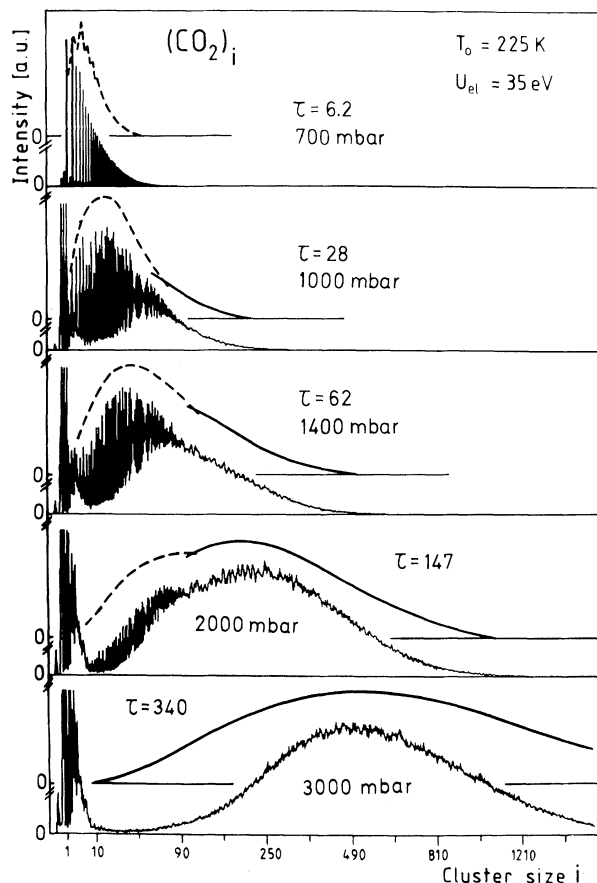


FIG. 1. Mass spectra of CO₂ clusters for increasing stagnation pressures p_0 , demonstrating the qualitative change in the size distributions. The ions which are visible in the left part ($i \leq 8$) of the high-pressure spectra are due to background gas, except for the monomer. The theoretical intensities were calculated by numerical integration of Eqs. (6) and multiplied by a factor proportional to the ionization cross section. Another factor proportional to \sqrt{i} was introduced for the unresolved parts of the spectra (solid lines, see text for explanation). For the resolved parts (dashed lines) this factor was not included. The value of the parameter τ , which measures the degree of coagulation, is fitted to achieve optimum accord with experiment in every spectrum.

monomer) are absent.¹⁹ Until now we have applied stagnation pressures up to 8000 mbar, resulting in a mean cluster ion size of $\langle i \rangle = 4100$ and zero intensity in the size range $2 \leq i \leq 1000$.

The model we have developed allows in general the fitting of the cluster size distribution as a function of a single parameter τ which measures the degree of condensation. The main assumption we make is that the supersaturation is high enough to neglect evaporations, as compared to condensations, for all cluster sizes. In other

words, we suppose that the critical cluster size reduces to the monomer. Then the kinetic equations for all cluster-cluster reactions are solved in general. These equations read²⁰

$$\frac{dn_k}{dt} = \sum_{\substack{i+j=k \\ i \leq j}} C_{ij} n_i n_j - \sum_i C_{ik} n_i n_k. \quad (1)$$

The first term on the right-hand side is the rate at which k -size clusters are formed by coagulation and the second term is the rate at which they are lost for the k size by growth to larger sizes. n_i is the concentration per unit volume of i -size clusters and the coefficients C_{ij} , which give the coagulation rate, read²¹

$$C_{ij} = 2\sigma_{ij} \left(\frac{2kT}{\pi} \right)^{1/2} \left(\frac{m_i + m_j}{m_i m_j} \right)^{1/2}. \quad (2)$$

m_i is the mass of an i -size cluster ($m_i = m_1 i$) and σ_{ij} is the total cross section for coagulation of an i -size cluster with a j -size cluster. If we assume a sticking coefficient of unity and a drop-let model of the clusters it simply reads $\pi(R_i + R_j)^2$ with $R_i = R_1 i^{1/3}$ being the radius of i -size clusters. The sticking coefficient of unity is well justified when the clusters become large because of the lower relative velocity and the existence of many vibrational modes into which the translational energy can be accommodated. Therefore

$$C_{ij}^* = \frac{C_{ij}}{C_{11}} = \frac{(i^{1/3} + j^{1/3})^2}{4\sqrt{2}} \left(\frac{i+j}{ij} \right)^{1/2}. \quad (3)$$

For a given $i+j$, these coefficients are larger the smaller is i and the larger is j or vice versa. This is because of the combination of the large cross section of one of the clusters and the high velocity of the other and explains why the smaller clusters disappear as soon as the larger ones are formed. Let $V(t)$ be the volume enclosing a macroscopic number N of molecules at time t and let N_i be the number of i -size clusters in the same volume. Now we make the following transformation of variables to have the kinetic equations dimensionless:

$$n_i^* = N_i/N, \quad (4)$$

and

$$\tau = \int_0^t 16\pi R_1^2 \left(\frac{kT(t')}{\pi m_1} \right)^{1/2} \frac{N}{V(t')} dt'. \quad (5)$$

Then Eq. (1) becomes

$$\frac{dn_k^*}{d\tau} = \sum_{\substack{i+j=k \\ i \leq j}} C_{ij}^* n_i^* n_j^* - \sum_i C_{ik}^* n_i^* n_k^*, \quad (6)$$

with the initial condition $n_i^* = \delta_{1i}$ for $\tau = 0$. Equa-

tions (1) and (6) appear in the context of aerosol coagulation kinetics²²⁻²⁷ and considerable progress has been achieved in their solution for a diffusion regime and for a free-molecule regime, as in our case. The nice result is that Eqs. (6) are independent of the particular conditions of the condensation process and even of the condensable gas. They can be solved once and forever, giving for any gas the relative concentrations n_i^* as a function of the parameter τ . Notice in Eq. (5) that, as the gas expands into the vacuum chamber, $V \rightarrow \infty$. Thus τ reaches a maximum value and the cluster distribution becomes frozen without evolving any more in time, as one would expect.

For comparison of the theory with the mass spectra, we corrected the calculated distributions with the size dependence of the ionization cross section, multiplying n_i^* by a factor proportional to $\sigma_i \propto i^{2/3}$ (cf. above). Also, as the spectra were recorded with a time-of-flight technique, the theoretical intensities dn_i^*/di had to be multiplied by an additional factor proportional to \sqrt{i} accounting for the time-to-mass conversion in the unresolved part of the spectrum. For the resolved part this factor must not be introduced since individual peaks are observed instead of density per unit time. In Fig. 1 we show the corrected theoretical intensities for the resolved (dashed line) and the unresolved (solid line) parts of the spectra. The agreement of these one-parameter fits is very good for $p_0 \geq 1000$ mbar. As apparent from the top spectrum in Fig. 1, the initial stages of the condensation process cannot be well described by our fit because of the assumption underlying Eq. (1), that is the neglect of the nucleation step. But this will be unimportant for latter times since any reasonable initial distribution will converge to the same "self-preserving" size distribution for large τ .²² A certain delay in the effective τ may occur, however. Deviation from experiment in the last spectrum may be due to the effect of attractive forces between the clusters²⁷ and more work will be needed in this direction.

There remains the problem of how the heat of condensation is evacuated from the clusters.²⁸ On this point it must be realized that the heat produced by the coagulation of an i cluster with a j cluster (with $i, j \gg 1$) is enormously less than the heat produced by the condensation of i monomers on a j cluster, as in steady-state nucleation. Therefore, after the cluster distribution has attained a certain size and most of the mass

is on clusters above that size, the coagulation can continue with relatively little production of heat. The clusters can transfer this internal heat to the beam translational energy by exchanging fast monomers: A monomer evaporated from a hot cluster will be recaptured by another cluster, at a lower mean relative velocity, and the system will gain relative momentum and lose internal energy. Only a small portion of monomers would be always present, just enough to deal with the extra heat produced by the coagulation at that moment. In fact, we observe experimentally that for high stagnation pressures 10% of the mass flux in the neutral beam is in the form of monomers. These may partly come from the monomers being exchanged, from interference of clusters with the skimmer and background gas, and from the evaporations of hot clusters during their free flight (about 1 ms) to the ionizer.²⁸

Two of us (J. M. S. and N. G.) would like to thank the IBM Research Laboratory at Zürich where the theory in this Letter was initiated. This work has been supported in part by the Comisión Asesora Científica y Técnica through Contract No. 4150/79 and by the Deutsche Forschungsgemeinschaft.

¹F. F. Abraham, *Homogeneous Nucleation Theory* (Academic, New York, 1974); J. Feder, K. C. Russel, J. Lothe, and G. M. Pound, *Adv. Phys.* **15**, 111 (1966); W. H. Zurek and W. C. Schieve, *Phys. Lett.* **67A**, 42 (1978).

²T. A. Milne and F. T. Greene, *J. Chem. Phys.* **47**, 4095 (1967); A. Hoareau, B. Cabaud, and P. Melinon, *Surf. Sci.* **106**, 195 (1981).

³C. G. Granqvist and R. A. Buhrman, *J. Appl. Phys.* **47**, 2200 (1976).

⁴T. Andersson and C. G. Granqvist, *J. Appl. Phys.* **48**, 1673 (1977).

⁵For a review, see G. S. Springer, *Adv. Heat Transf.* **14**, 281 (1978).

⁶R. Becker and W. Döring, *Ann. Phys. (Leipzig)* **24**, 719 (1935); N. García and J. M. Soler, *Phys. Rev. Lett.* **47**, 186 (1981).

⁷The nonsteady state was studied by F. F. Abraham, *J. Chem. Phys.* **51**, 1632 (1969), by integrating the kinetic equations in time but without considering cluster-cluster collisions.

⁸See, e.g., D. Dreyfuss and H. Y. Wachman, *J. Chem.*

Phys. **76**, 2031 (1982), and references therein.

⁹W. Henkes and G. Isenberg, *Int. J. Mass Spectrom. Ion Phys.* **5**, 249 (1970); J. Gspann and K. Körting, *J. Chem. Phys.* **59**, 4726 (1973); W. Henkes, V. Hoffman, and F. Mikosch, *Rev. Sci. Instrum.* **48**, 675 (1977).

¹⁰J. Gspann and H. Vollmar, *J. Chem. Phys.* **73**, 1657 (1980).

¹¹K. Sattler, J. Mühlbach, O. Echt, P. Pfau, and E. Recknagel, *Phys. Rev. Lett.* **47**, 160 (1981).

¹²O. Echt, K. Sattler, and E. Recknagel, *Phys. Lett.* **90A**, 185 (1982).

¹³J. K. Lee, J. A. Barker, and F. F. Abraham, *J. Chem. Phys.* **58**, 3166 (1973); C. L. Briant and J. J. Burton, *J. Chem. Phys.* **63**, 2045 (1975); see also the review by M. R. Hoare, *Adv. Chem. Phys.* **40**, 49 (1979).

¹⁴O. F. Hagena and W. Obert, *J. Chem. Phys.* **56**, 1793 (1972).

¹⁵K. Sattler, J. Mühlbach, E. Recknagel, and A. Reyes-Flotte, *J. Phys. E* **13**, 673 (1980).

¹⁶H. Falter, O. F. Hagena, W. Henkes, and H. v. Wedel, *Int. J. Mass Spectrom. Ion Phys.* **4**, 145 (1970).

¹⁷E. N. Nikolaev, G. D. Tantsyrev, and V. A. Saraev, *Zh. Tekh. Fiz.* **23**, 406 (1978) [*Sov. Phys. Tech. Phys.* **23**, 241 (1978)].

¹⁸In the spectra with $p_0 \geq 1000$ mbar, the individual peaks in this band are modulated by interferencelike effects, caused by the finite number of channels available for each spectrum. This does not, however, affect the envelope of the spectra which will be compared with the theoretical size distribution.

¹⁹The ions which are visible in the left part ($i \leq 8$) of the high-pressure spectra in Fig. 1 are due to background gas; they disappeared after baking the apparatus. The origin of the monomers will be discussed later.

²⁰M. Smoluchowski, *Z. Phys. Chem.* **92**, 129 (1918).

²¹S. Chapman and T. G. Cowling, *The Mathematical Theory of Nonuniform Gases* (Cambridge Univ. Press, Cambridge, England, 1970).

²²F. S. Lai, S. K. Friedlander, J. Pich, and G. M. Hidy, *J. Colloid Interface Sci.* **39**, 395 (1972).

²³P. Middleton and J. Brock, *J. Colloid Interface Sci.* **54**, 249 (1976).

²⁴S. H. Suck and J. R. Brock, *J. Aerosol Sci.* **10**, 581 (1979).

²⁵F. Gelbard and J. H. Seinfeld, *J. Colloid Interface Sci.* **78**, 485 (1980).

²⁶S. C. Graham and J. B. Homer, *Faraday Symp. Chem. Soc.* **7**, 7 (1973).

²⁷W. H. Marlow, *J. Chem. Phys.* **73**, 6284-6295 (1980).

²⁸J. M. Soler and N. García, *Phys. Rev. A*, to be published.